

Cannabinoids suppress inflammatory and neuropathic pain by targeting $\alpha 3$ glycine receptors

Wei Xiong,¹ Tanxing Cui,^{3,4,5} Kejun Cheng,² Fei Yang,⁶ Shao-Rui Chen,⁷ Dan Willenbring,^{3,4,5} Yun Guan,⁶ Hui-Lin Pan,⁷ Ke Ren,⁸ Yan Xu,^{3,4,5} and Li Zhang¹

¹Laboratory for Integrative Neuroscience, National Institute on Alcohol Abuse and Alcoholism, and ²Chemical Biological Research Branch, National Institute on Drug Abuse, National Institutes of Health, Bethesda, MD 20892

³Department of Anesthesiology, ⁴Department of Pharmacology & Chemical Biology, and ⁵Department of Structural Biology, University of Pittsburgh School of Medicine, Pittsburgh, PA 15213

⁶Department of Anesthesiology and Critical Care Medicine, Johns Hopkins University, School of Medicine, Baltimore, MD 21205

⁷Center for Neuroscience and Pain Research, Department of Anesthesiology and Perioperative Medicine, The University of Texas MD Anderson Cancer Center, Houston, TX 77030

⁸Department of Neural and Pain Sciences, University of Maryland Dental School, Baltimore, MD 21201

Certain types of nonpsychoactive cannabinoids can potentiate glycine receptors (GlyRs), an important target for nociceptive regulation at the spinal level. However, little is known about the potential and mechanism of glycinergic cannabinoids for chronic pain treatment. We report that systemic and intrathecal administration of cannabidiol (CBD), a major nonpsychoactive component of marijuana, and its modified derivatives significantly suppress chronic inflammatory and neuropathic pain without causing apparent analgesic tolerance in rodents. The cannabinoids significantly potentiate glycine currents in dorsal horn neurons in rat spinal cord slices. The analgesic potency of 11 structurally similar cannabinoids is positively correlated with cannabinoid potentiation of the $\alpha 3$ GlyRs. In contrast, the cannabinoid analgesia is neither correlated with their binding affinity for CB1 and CB2 receptors nor with their psychoactive side effects. NMR analysis reveals a direct interaction between CBD and S296 in the third transmembrane domain of purified $\alpha 3$ GlyR. The cannabinoid-induced analgesic effect is absent in mice lacking the $\alpha 3$ GlyRs. Our findings suggest that the $\alpha 3$ GlyRs mediate glycinergic cannabinoid-induced suppression of chronic pain. These cannabinoids may represent a novel class of therapeutic agents for the treatment of chronic pain and other diseases involving GlyR dysfunction.

CORRESPONDENCE

Li Zhang:
lzhang@mail.nih.gov

Abbreviations used: CBD, cannabidiol; DD-CBD, didesoxy-CBD; DH-CBD, dehydroxyl-CBD; GlyR, glycine receptor; HSQC, heteronuclear single quantum coherence; i.t., intrathecal; LPPG, lyso-1-palmitoylphosphatidylglycerol; NOESY, nuclear Overhauser effect spectroscopy; PGE₂, prostaglandin E₂; PWL, paw withdrawal latency; PWT, paw withdrawal threshold; SNL, spinal nerve injury; THC, tetrahydrocannabinol.

Chronic pain, particularly neuropathic pain, is a major clinical problem that is difficult to treat (Zhuo, 2007). Despite an intensive search for new analgesics in the last several decades, the need for novel therapeutic strategies remains unmet because virtually every blockbuster drug for the treatment of chronic pain produces aversive side effects (Mogil, 2009; Harrison, 2011). Marijuana has been used to treat chronic pain for thousands of years (Burns and Ineck, 2006; Murray et al., 2007). However, the widespread use of medical marijuana is still controversial because the plant produces both therapeutic and psychoactive effects. Marijuana consists of ~400 chemical compounds, and ~60 of them are structurally related cannabinoids. Δ^9 -tetrahydrocannabinol (THC) and cannabidiol (CBD) among cannabinoids are major psychoactive and nonpsychoactive

components of marijuana, respectively (Howlett et al., 2002; Costa, 2007). There is strong evidence suggesting that nonpsychoactive cannabinoids can also alleviate chronic inflammatory and neuropathic pain in animals (Costa et al., 2007; Izzo et al., 2009). Several recent clinical studies have demonstrated that combination of THC and CBD can be an effective therapeutic option for patients with neuropathic pain and other types of chronic pain (Nurmikko et al., 2007; Turcotte et al., 2010; Lynch and Campbell, 2011). However, there is a need to improve the efficacy and tolerability of these agents in treating

© 2012 Xiong et al. This article is distributed under the terms of an Attribution-Noncommercial-Share Alike-No Mirror Sites license for the first six months after the publication date (see <http://www.rupress.org/terms>). After six months it is available under a Creative Commons License (Attribution-Noncommercial-Share Alike 3.0 Unported license, as described at <http://creativecommons.org/licenses/by-nc-sa/3.0/>).

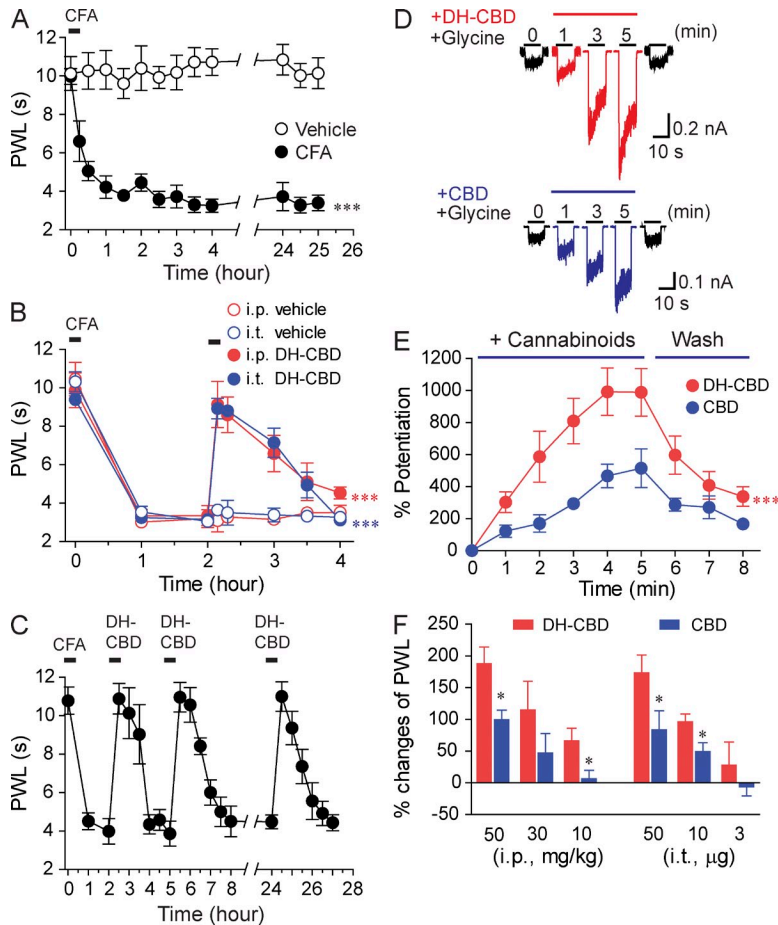


Figure 1. Suppression of inflammatory pain by CBD and DH-CBD in mice. (A) Time course of heat pain hypersensitivity in mice after 20 μ l CFA paw injection (1:4 in saline). Each data point represents the mean from 10–15 mice. (B) The analgesic effect of i.p. (50 mg/kg, $n = 10$) and i.t. (50 μ g, $n = 10$) injection of DH-CBD or vehicle in mice 2 h after CFA injection. (C) The analgesic effect of the repeated application of i.p. injection of 50 mg/kg DH-CBD ($n = 10$) in mice after CFA injection. Note that the analgesic effect was nearly identical after repeated applications of DH-CBD during a period of two consecutive days after CFA injection. (D) Traces of I_{Gly} in the absence and presence of 1 μ M DH-CBD and 1 μ M CBD in HEK 293 cells expressing the $\alpha 3$ GlyRs. (E) Time course of CBD- ($n = 7$) and DH-CBD ($n = 9$)-induced potentiation on I_{Gly} in HEK 293 cells expressing the $\alpha 3$ GlyRs. (F) Dose-dependent analgesic effects of CBD ($n = 10$) and DH-CBD ($n = 10$) applied i.p. and i.t. in mice with CFA paw injection. Data are representative of two to three independent experiments (*, $P < 0.05$; ***, $P < 0.001$) and expressed as mean \pm SEM.

chronic pain. One primary obstacle to development of these agents is the uncertainty about the molecular targets for cannabinoid-induced analgesic effects. For instance, the role of spinal CB1 receptors (CB1Rs) in the pain process is debatable. Some studies suggest that activation of CB1Rs in the spinal dorsal horn can facilitate pain (Pernía-Andrade et al., 2009; Zhang et al., 2010; Zeilhofer et al., 2012). Notably, THC-induced analgesia in the tail flick reflex, a test for nociceptive pain threshold, remains intact in mice devoid of CB1 receptors (CB1 $^{-/-}$; Zimmer et al., 1999; Howlett et al., 2002).

Recent studies have shown that glycine receptors (GlyRs) are an important target for cannabinoids in the central nervous system. For instance, several synthetic and phytocannabinoids, including THC and CBD, can potentiate glycine currents (I_{Gly}) in native neurons isolated from the ventral tegmental area, amygdala, hippocampus, and spinal cord and in various heterologous cells expressing recombinant GlyRs (Hejazi et al., 2006; Yang et al., 2008; Ahrens et al., 2009a,b; Demir et al., 2009; Foadi et al., 2010; Xiong et al., 2011, 2012; Yevenes and Zeilhofer, 2011a,b). GlyRs are thought to play an important role in the antinociceptive process (Harvey et al., 2004, 2009; Zeilhofer, 2005; Lynch and Callister, 2006; Pernía-Andrade et al., 2009; Zeilhofer et al., 2012). There are four isoforms of the α subunits ($\alpha 1$ – $\alpha 4$) and a single isoform of the β subunit. The adult form of GlyRs are composed of α and β subunits in a pentameric

assembly (Lynch, 2004). The role of the $\alpha 3$ subunit in modulating inflammatory pain has been the focus of many discussions. The $\alpha 3$ -containing GlyRs are abundantly located in the lamina II of the spinal dorsal horn, an area known for integrating nociceptive information. Experimental evidence suggests that prostaglandin E_2 (PGE $_2$), a critical mediator of central and peripheral pain sensitization, selectively inhibits the $\alpha 3$ GlyR function (Ahmadi et al., 2002; Harvey et al., 2004, 2009). Such disinhibition of the $\alpha 3$ GlyRs is found to contribute to the mechanism of chronic inflammatory pain induced by the intraplantar injection of CFA (Harvey et al., 2004, 2009).

Our recent study suggests that cannabinoid potentiation of GlyRs can produce a potent analgesic effect in mice (Xiong et al., 2011). The idea was mainly based on the results obtained in the tail flick test, a measure of transient nociception which only resembles the normal physiological state (Grossman et al., 1982). It is important to determine whether allosteric facilitation of GlyRs by cannabinoids contributes to the treatment of pathological or chronic pain states. Here, we demonstrate that glycinergic cannabinoids suppress inflammatory and neuropathic pain without significantly causing major psychoactive side effect and analgesic tolerance. The suppression of pathological pain by glycinergic cannabinoids is mediated through an $\alpha 3$ GlyR-dependent mechanism. We also provide mechanistic details of drug–receptor interaction and strategies for future studies to develop a new generation of glycinergic cannabinoid-based agents for the treatment of chronic pain and other diseases involving GlyR dysfunction.

RESULTS

Glycinergic cannabinoids suppress persistent inflammatory pain in both mice and rats

Previous studies have shown that both CBD and dehydroxyl-CBD (DH-CBD) potentiated I_{Gly} in HEK 293 cells expressing

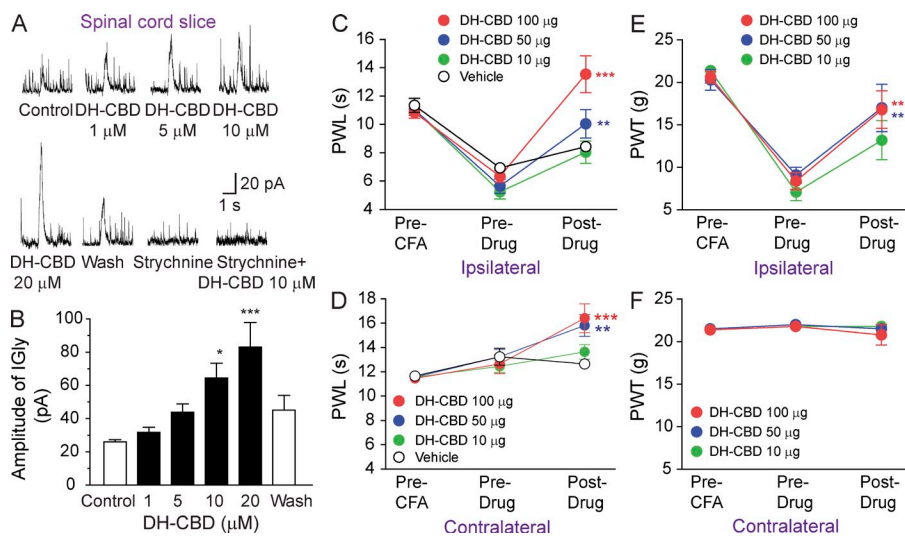


Figure 2. DH-CBD potentiation of I_{Gly} in spinal neurons and suppression of inflammatory pain in rats. (A) Original recordings showing currents activated by puff application of 30 μ M glycine to lamina II neurons with and without sustained DH-CBD application in rat spinal cord slices. 1 μ M strychnine, a specific GlyR antagonist, was used to determine whether GlyRs are the target that mediates the DH-CBD-induced potentiation. (B) Bar graphs of DH-CBD-induced potentiation on I_{Gly} of spinal lamina II neurons ($n = 7$). (C and D) Effect of i.t. application of DH-CBD or vehicle on the ipsilateral (C) and contralateral (D) PWL to noxious heat stimulation in rats before and after intraplantar CFA injection ($n = 6-7$). (E and F) As in C and D, but rats were subjected to punctuate mechanical stimuli ($n = 8$). Data are representative of three (A and B) and two (C-F) independent experiments (*, $P < 0.05$; **, $P < 0.01$; ***, $P < 0.001$, post-drug vs. pre-drug) and expressed as mean \pm SEM.

the $\alpha 1$ and $\alpha 3$ subunits (Ahrens et al., 2009a; Xiong et al., 2011). In view of this, we first examined the effect of DH-CBD and CBD on inflammatory pain induced by intraplantar injection of 20 μ l CFA (1:4 in saline) into one hind paw of the mice. CFA induced prolonged hypersensitivity to thermal pain in mice, reflected by a significant decrease in paw withdrawal latency (PWL) upon exposure to heat stimulus (Fig. 1 A, $P < 0.001$). The magnitude of CFA-induced persistent pain reached maximum 2 h after injection and persisted throughout the observation period in mice. i.p (50 mg/kg) and intrathecal (i.t.; 50 μ g) administration of DH-CBD caused a significant increase in the PWL (Fig. 1 B). The increase in the PWL developed and peaked within the 1st h, and persisted for 2 h. DH-CBD-induced analgesia was fully replicated at multiple times within the same day or next day (Fig. 1 C). This suggests that there is no apparent tolerance with DH-CBD-induced analgesia. In HEK 293 cells expressing the $\alpha 3$ GlyRs, DH-CBD was more efficacious than CBD in potentiating I_{Gly} (Fig. 1 D). For instance, the maximal magnitude of DH-CBD (1 μ M)-induced potentiation was $989 \pm 171\%$, whereas the magnitude of CBD-induced potentiation was $491 \pm 101\%$ (Fig. 1 E). These values are significantly different ($P < 0.01$). Both DH-CBD and CBD given i.p. or i.t. increased PWL in a dose-dependent manner (Fig. 1 F). Consistent with the observation of in vitro study that DH-CBD was more efficacious than CBD in potentiating I_{Gly} , DH-CBD was more potent than CBD in alleviating heat pain hypersensitivity (Fig. 1 F).

Next, we examined whether or not DH-CBD can potentiate I_{Gly} in rat spinal dorsal horn neurons and whether or not i.t. application of DH-CBD can attenuate inflammatory thermal and mechanical pain hypersensitivity in rats. DH-CBD at concentrations from 1 to 20 μ M increased the amplitudes of I_{Gly} of lamina II neurons, produced by puff application of 30 μ M glycine in rat spinal cord slices (Fig. 2, A and B). This potentiation appeared dependent on the concentrations of DH-CBD and required sustained application of DH-CBD for at least 6 min to reach a peak. The DH-CBD-induced potentiation of I_{Gly} was

maximal at the lowest concentrations of glycine. DH-CBD did not significantly alter the amplitude of current activated by glycine at concentrations equal to or higher than 300 μ M (unpublished data). The specific GlyR antagonist strychnine completely abolished I_{Gly} and the potentiation of DH-CBD (Fig. 2 A), suggesting that the native GlyRs are the target that mediates the DH-CBD-induced potentiation.

Consistent with the observation in the previous paragraph, the ipsilateral PWLs were significantly decreased from the preinflammation baselines in rats at days 1-3 after receiving an intraplantar injection of CFA into the left hind paw (Fig. 2 C, $P < 0.01$). We then injected rats i.t. with DH-CBD (10 μ g/15 μ l, 50 μ g/15 μ l, or 100 μ g/15 μ l) or vehicle, and PWL was measured again at 30-60 min after injection. DH-CBD dose-dependently increased the ipsilateral PWL from preinjection values (Fig. 2 C, 50 μ g: $P < 0.01$, 100 μ g: $P < 0.001$) and also increased the contralateral PWLs from the preinflammation baselines at 50 μ g ($P < 0.01$) and 100 μ g ($P < 0.01$) doses (Fig. 2 D). The ipsilateral paw withdrawal thresholds (PWTs) to punctuate mechanical stimuli were significantly decreased from preinflammation baselines in rat at day 1-3 after intraplantar injection of CFA (Fig. 2 E, $P < 0.001$). The ipsilateral PWTs were significantly increased at 30-60 min after i.t. injection of DH-CBD at 50 μ g ($P < 0.01$) and 100 μ g ($P < 0.01$) doses, but not at a 10 μ g dose (Fig. 2 E, $P = 0.075$). The contralateral PWTs were not significantly changed (Fig. 2 F).

DH-CBD suppress chronic neuropathic pain

Peripheral nerve injury can cause clinically relevant chronic neuropathic pain (Guan et al., 2008). The fifth lumbar spinal nerve injury (SNL) produced long-lasting mechanical and thermal hypersensitivity on the ipsilateral hind paw in rats (Fig. 3, A and C). The PWTs to the application of calibrated von Frey filaments to the plantar side of the hind paw ipsilateral to the nerve injury significantly decreased from the preinjury baseline values, a behavioral indication

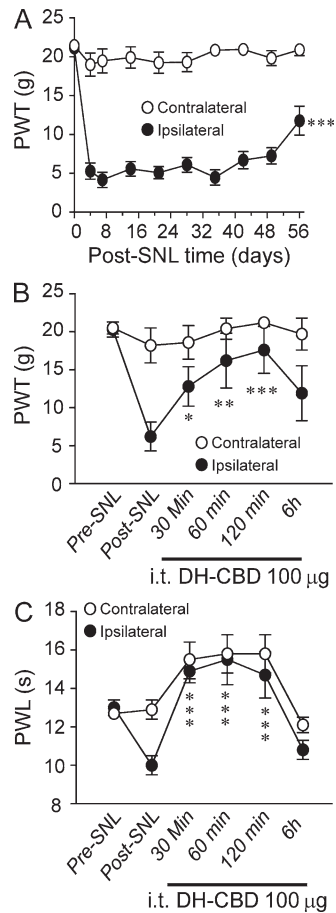


Figure 3. DH-CBD suppression of neuropathic pain in rats. (A) Time courses of the ipsilateral and contralateral PWT to mechanical stimulation after the fifth lumbar SNL in rats ($n = 12$). ***, $P < 0.001$, as compared with pre-SNL. (B and C) The analgesic effect of i.t. application of DH-CBD at 100 μg on PWT to mechanical stimulation (B) or heat stimulation (C) on day 14 after SNL ($n = 12$). *, $P < 0.05$; **, $P < 0.01$; ***, $P < 0.001$, as compared with pre DH-CBD. Data are representative of three independent experiments and expressed as mean \pm SEM.

of mechanical hypersensitivity. The mechanical hypersensitivity appeared on day 3, reached a peak level between days 7 and 14, and persisted for at least 4 wk after nerve injury ($P < 0.001$). In rats at days 12–14 after SNL, i.t. administration of 100 μg DH-CBD significantly attenuated mechanical pain hypersensitivity (Fig. 3 B). The ipsilateral PWTs were significantly increased from the preinjection level at 30, 60, and 120 min after DH-CBD injection (Fig. 3 B, $P < 0.05$). The contralateral PWTs were not significantly changed. We then examined the effect of DH-CBD on heat pain hypersensitivity in nerve-injured rats. In rats at days 12–14 after SNL, the ipsilateral PWLs were significantly decreased from the pre-SNL baselines (Fig. 3 C, $P < 0.05$) but were significantly increased at 30–120 min after i.t. administration of DH-CBD (Fig. 3 C, 100 $\mu\text{g}/15 \mu\text{l}$; $P < 0.001$). The drug effect was largely diminished by 6 h after injection. DH-CBD at this dose also significantly increased the contralateral PWL from pre-SNL baseline at 60 and 120 min after injection.

DH-CBD rescues PGE₂-induced inhibition of $\alpha 3$ GlyR activity and i.t. PGE₂-induced persistent pain

PGE₂ is one of the major proinflammatory substances that promote nociceptive processing in the spinal cord upon various noxious stimuli (Vanegas and Schaible, 2001; Zeilhofer et al., 2012). There is also evidence to suggest that the PGE₂ signaling pathway critically contributes to pain hypersensitivity after peripheral nerve injury (Marchand et al., 2005; Patapoutian et al., 2009). A previous study has suggested that elevated PGE₂ promotes nociceptive action through inhibiting spinal $\alpha 3$ GlyR function (Harvey et al., 2004). We proposed that the spinal $\alpha 3$ GlyR is the target for the cannabinoid-induced analgesic effect. A legitimate question remains as to whether or not cannabinoids can modulate the $\alpha 3$ GlyRs upon activation of PGE₂ receptors (EP2Rs). To address this question, we coexpressed the $\alpha 3$ GlyRs with EP2Rs in HEK 293 cells. In these cells, preincubation with 10 μM PGE₂ significantly reduced the amplitude of current activated by 200 μM (EC₂₀) glycine (Fig. 4, A and B). In contrast, PGE₂ did not significantly alter I_{Gly} in cells coexpressing EP2Rs and $\alpha 1$ GlyRs. These findings are consistent with the observations described in a previous study (Harvey et al., 2004). The PGE₂ inhibition of the $\alpha 3$ GlyRs developed slowly and reached the maximal 5–8 min after application of PGE₂ (Fig. 4 B). In the same cells with continuous incubation of PGE₂, DH-CBD at 1 μM significantly potentiated I_{Gly} (Fig. 4, C and D, $P < 0.001$).

i.t. application of PGE₂ (0.2 nmol per mouse) induced persistent thermal pain hypersensitivity (Fig. 4 E). Consistent with a previous study (Harvey et al., 2004), $\alpha 3$ GlyR knockout ($\alpha 3^{-/-}$) mice showed a complete lack of pain sensitization compared with WT littermates (Fig. 4 E, $P < 0.001$), suggesting an involvement of the $\alpha 3$ GlyRs in spinal PGE₂-dependent pain signaling pathway. DH-CBD completely reversed the reduction in PWL induced by i.t. PGE₂ in mice (Fig. 4 F; $P < 0.001$).

Didesoxy-CBD (DD-CBD) inhibits DH-CBD-induced potentiation of I_{Gly} and analgesic effect

Consistent with our recent observations (Xiong et al., 2011, 2012), chemically modified CBD with removal of both hydroxyl and oxygen groups (DD-CBD) did not significantly alter the amplitude of I_{Gly} in HEK 293 cells expressing the $\alpha 3$ GlyRs (Fig. 5 A). In these cells, DD-CBD inhibited the DH-CBD (1 μM)-induced potentiation on I_{Gly} in a concentration-dependent manner (Fig. 5, A and B). DD-CBD at 3 μM shifted in a parallel manner the concentration-response curve of DH-CBD-induced potentiation of the $\alpha 3$ GlyRs to the right (Fig. 5 C). We next examined whether or not DD-CBD can inhibit DH-CBD-induced analgesic effect in persistent pain. Although systemic or i.t. application of DD-CBD (50 mg/kg i.p. or 10 μg i.t.) alone did not significantly alter the PWL in CFA-treated mice (Fig. 5 D), DD-CBD when applied either i.t. or i.p. antagonized the DH-CBD (50 mg/kg i.p.)-induced analgesic effect in CFA-induced pain hypersensitivity in mice (Fig. 5, E and F). This DD-CBD-induced antagonism appeared to be dose dependent and reached the maximal magnitude (complete inhibition of DH-CBD-induced analgesia) when applied at 10 mg/kg i.p. or 10 μg i.t. ($P < 0.001$).

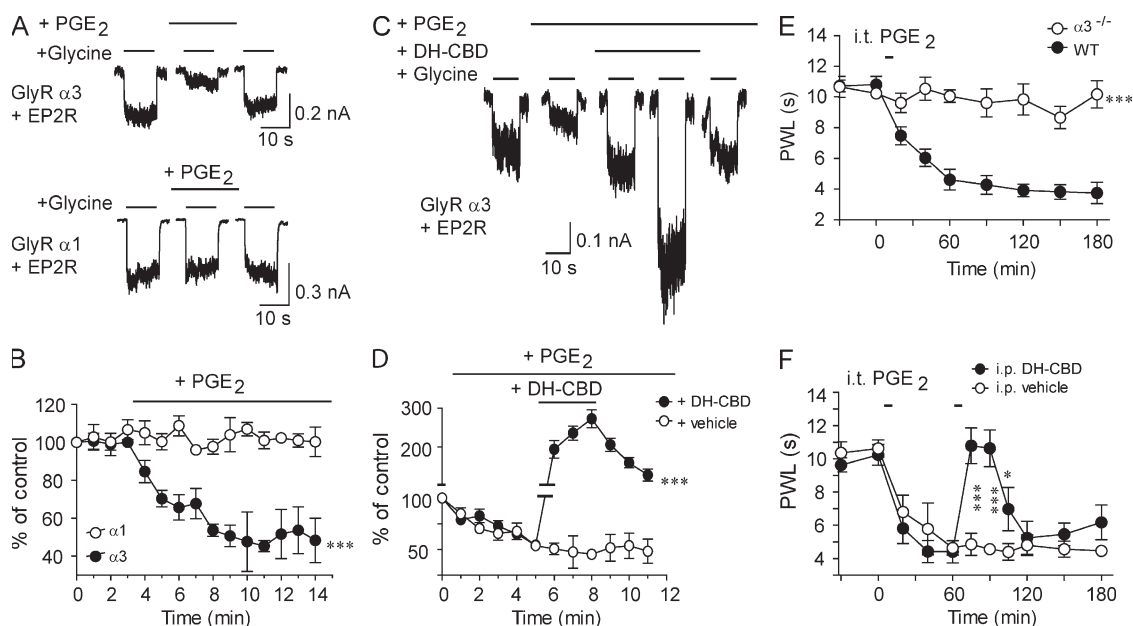


Figure 4. DH-CBD rescue of PGE₂-induced inhibition of the α 3 GlyRs and chronic pain. (A) Trace records of I_{Gly} in HEK 293 cells coexpressing EP2 receptors with either the α 3 or α 1 GlyRs before and after sustained PGE₂ application. (B) Time courses of I_{Gly} in the cells coexpressing EP2 receptors with either the α 3 ($n = 6$) or α 1 ($n = 5$) GlyRs after sustained PGE₂ application. ***, $P < 0.001$ (α 1 vs. α 3). (C) Trace records of I_{Gly} in cells coexpressing EP2 receptors with the α 3 GlyRs without and with DH-CBD after sustained PGE₂ application. (D) Time courses of DH-CBD potentiation of I_{Gly} in cells coexpressing the α 3 GlyRs and EP2Rs after sustained PGE₂ application ($n = 6$). ***, $P < 0.001$ as compared with vehicle application. (E) Time courses of PWL to thermal stimulation before, during, and after i.t. PGE₂ injection in WT and α 3^{-/-} mice ($n = 10$). ***, $P < 0.001$, as compared with the WT mice. (F) The analgesic effect of 50 mg/kg DH-CBD i.p. ($n = 10$) on PWL to thermal stimulation after i.t. PGE₂ injection. *, $P < 0.05$; ***, $P < 0.001$, as compared with i.p. vehicle ($n = 10$). Data are representative of two independent experiments and expressed as mean \pm SEM.

The α 3 GlyR is essential for the DH-CBD-induced analgesic effect in chronic pain

To date, there is no antagonist highly selective for a specific GlyR subunit. The α 3^{-/-} mice have been shown to be valuable for exploring the α 3 GlyR-mediated behaviors (Harvey et al., 2004, 2009; Hösl et al., 2006; Manzke et al., 2010; Xiong et al., 2011). To study the role of the α 3 subunit in CBD and DH-CBD-induced analgesia, we conducted the following experiments using the α 3^{-/-} mice. We observed that both CBD and DH-CBD-induced analgesic effects in CFA-induced pain hypersensitivity were significantly reduced in mice lacking the α 3 subunits as compared with the WT littermates (Fig. 6, A and B). For instance, the peak values of PWL after CBD and DH-CBD (50 mg/kg i.p.) were 8.1 ± 0.5 and 10.7 ± 0.6 s in the WT mice, whereas the peak values of PWL after CBD and DH-CBD were 4.3 ± 0.7 and 5.9 ± 0.8 s in α 3^{-/-} mice. The values between the WT and α 3^{-/-} mice are significantly different ($P < 0.001$). Both CBD- and DH-CBD-induced analgesic effects remained unchanged in either CB1 knockout mice (Fig. 6, C and D) or CB2 knockout mice as compared with their WT littermates (Fig. 6, E and F).

Correlation analysis: cannabinoid potentiation of I_{Gly} is correlated with cannabinoid-induced analgesic potency

Fig. S1 lists the names and chemical structures of 11 synthetic cannabinoids structurally similar to CBD. We explored the structural and functional activity of these cannabinoids by

measuring the following functional indexes: the binding affinity of the cannabinoids bound for both CB1 receptors (in purified brain membrane) and CB2 receptors (in purified CB2 receptor protein from transformed *Escherichia coli* bacteria cells), the potentiation of I_{Gly} induced by 1 μ M cannabinoids and the EC₅₀ values of cannabinoid potentiation of I_{Gly} in HEK 293 cells expressing the α 3 GlyRs, and cannabinoid-induced analgesic effect in CFA-induced inflammatory pain in mice. Although these cannabinoids share a high degree of structural similarity, they differed significantly in their binding affinity for CB1/CB2 receptors, their potencies in potentiating I_{Gly} , and their inhibition of pain hypersensitivity in mice (Fig. S1). Except for inducing an analgesic effect, some of these cannabinoids, such as THC and HU210, substantially reduced body temperature, locomotor activity, and balance and coordination skills in mice (Fig. 7). There was a strong correlation between the cannabinoid-induced potentiation of I_{Gly} and cannabinoid-induced analgesic effect in chronic inflammatory pain in mice (Fig. 7 A, 1 μ M cannabinoid-induced potentiation vs. i.p. 50 mg/kg cannabinoid-induced percentage changes of PWL, $P < 0.001$). There was also a strong correlation between the EC₅₀ values of cannabinoid potentiation of I_{Gly} and cannabinoid-induced percentage changes of PWL ($r^2 = 0.662$, $P < 0.05$). In contrast, the magnitudes of cannabinoid-induced analgesia in chronic pain were not significantly correlated with the binding affinity of cannabinoids

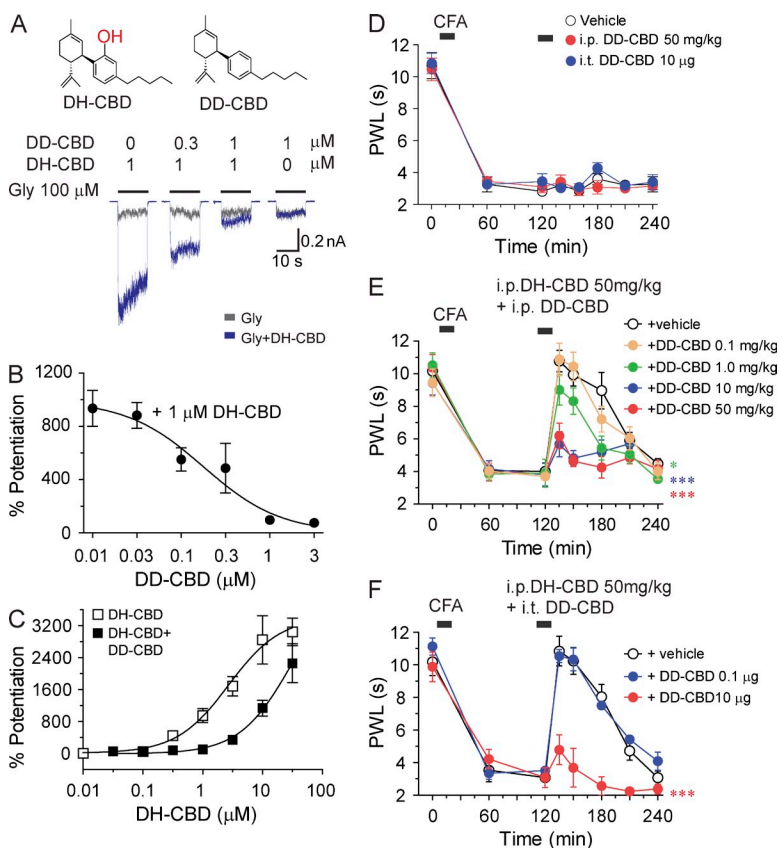


Figure 5. Antagonism of DD-CBD to DH-CBD-induced potentiation of I_{Gly} and analgesia in inflammatory pain.

(A) Structures of DH-CBD and DD-CBD. Trace records of I_{Gly} in HEK 293 cells expressing the $\alpha 3$ GlyRs without and with co-application of DD-CBD and DH-CBD. (B) DD-CBD inhibition of DH-CBD-induced potentiation of I_{Gly} in HEK 293 cells expressing the $\alpha 3$ GlyRs ($n = 6$). (C) The concentration-response curves of DH-CBD-induced potentiation of I_{Gly} without and with $1 \mu M$ DD-CBD ($n = 5-7$). (D) The effect of i.t. and i.p. application of DD-CBD on PWL to thermal stimulation after CFA paw injection in mice ($n = 7-10$). (E) Dose-dependent inhibition of i.p. DH-CBD-induced analgesic effect by i.p. application of DD-CBD in post-CFA mice ($n = 7-10$). (F) Dose-dependent inhibition of i.p. DH-CBD-induced analgesic effect by i.t. application of DD-CBD in post-CFA mice ($n = 8-10$). *, $P < 0.05$; ***, $P < 0.001$, as compared with vehicle injection. Data are representative of two independent experiments and expressed as mean \pm SEM.

effects such as hypothermia, hypolocomotion, and incoordination ($P > 0.05$).

NMR analysis: a direct interaction between CBD and the S296-containing domain of the $\alpha 3$ GlyR

Our recent study using NMR analysis has revealed chemical shift of the S296 residue in the TM3 of purified $\alpha 1$ GlyR-TM proteins by THC titration (Xiong et al., 2011). However, there are two unsolved issues. First, it is unclear if cannabinoids can interact with the $\alpha 3$ GlyR, as the

previous experiment was conducted with the $\alpha 1$ GlyR TM domains. There are 12 residues different within the four TM domains between the $\alpha 1$ and $\alpha 3$ subunits. Second, changes in chemical shift, although indicative of cannabinoid-receptor

for either CB1 or CB2 receptors (Fig. 7, C and D, $P > 0.05$). Neither cannabinoid-induced potentiation of GlyRs (Fig. 7, D-F) nor cannabinoid-induced analgesia (Fig. 7, G-I) was significantly correlated with cannabinoid-induced psychoactive

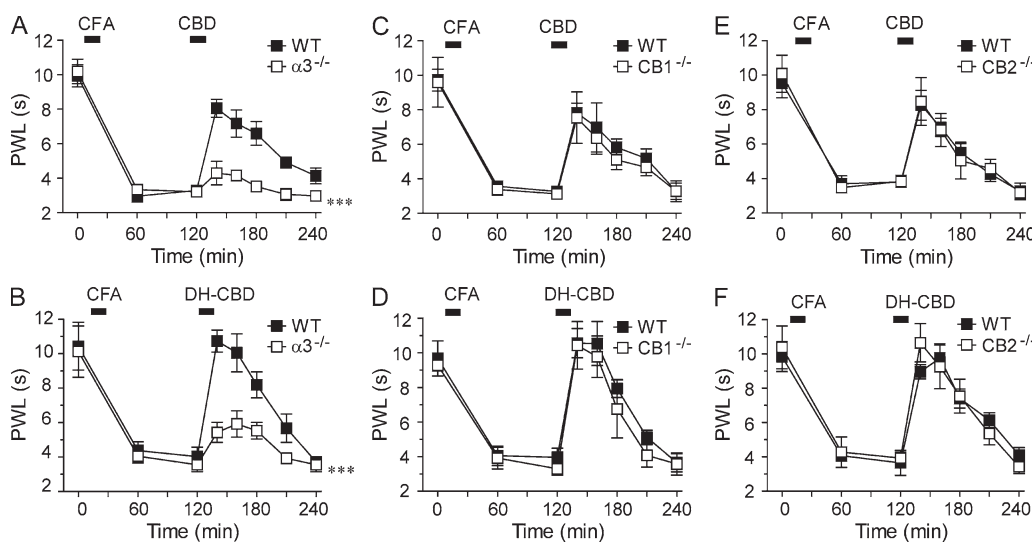


Figure 6. A decrease in CBD and DH-CBD-induced analgesia in the $\alpha 3^{-/-}$ mice but not in the $CB1^{-/-}$ and $CB2^{-/-}$ mice. (A and B) The analgesic effect of 50 mg/kg CBD i.p. (A) or 50 mg/kg DH-CBD i.p. (B) on PWL to thermal stimulation after CFA injection in the $\alpha 3^{-/-}$ mice ($n = 9-10$). ***, $P < 0.001$, as compared with WT mice. (C and D) The analgesic effect of 50 mg/kg CBD i.p. (C) or 50 mg/kg DH-CBD i.p. (D) on PWL to thermal stimulation after CFA injection in the $CB1^{-/-}$ mice ($n = 6$). (E and F) The analgesic effect of 50 mg/kg CBD i.p. (E) or 50 mg/kg DH-CBD i.p. (F) on PWL to thermal stimulation after CFA injection in the $CB2^{-/-}$ mice ($n = 6$). Data are representative of two independent experiments and expressed as mean \pm SEM.

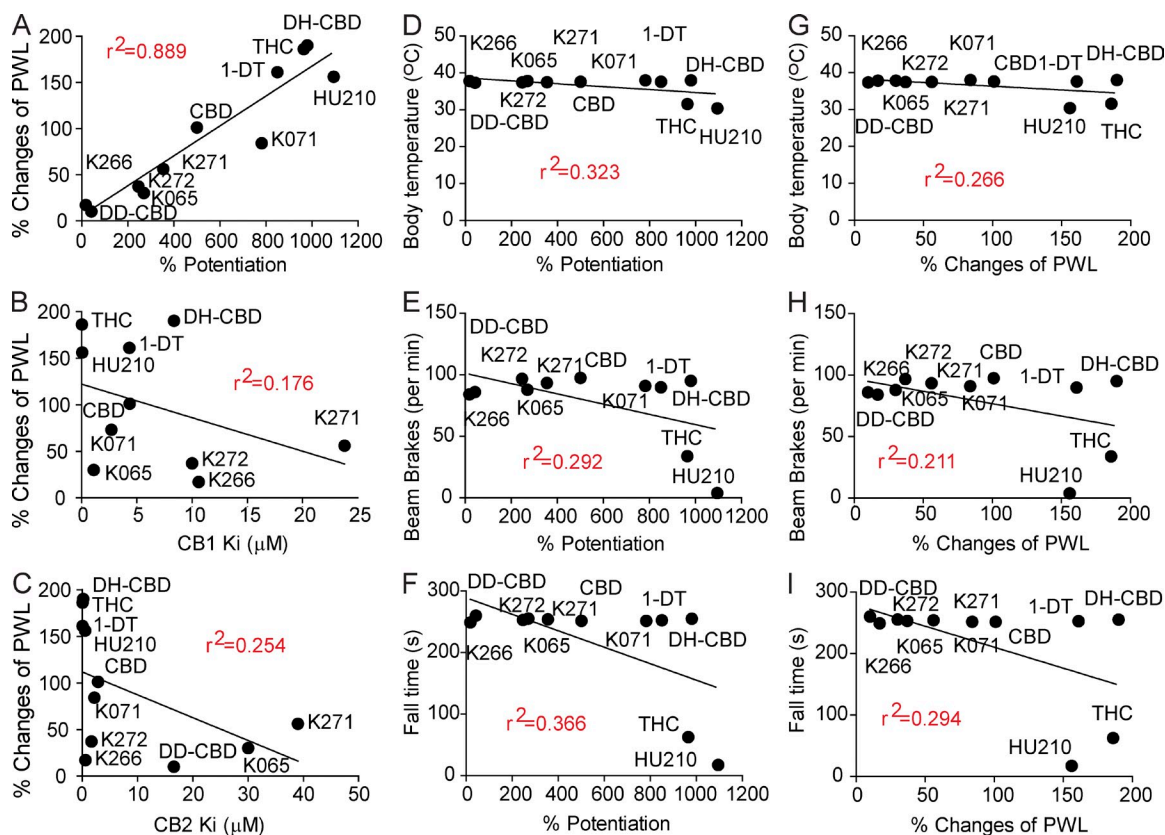


Figure 7. Correlation analysis: relationships between cannabinoid potentiation and cannabinoid-induced analgesic and psychoactive effects. Correlation analysis: (A) Cannabinoid (1 μM)-induced potentiation of I_{Gly} versus the analgesic potency (percent changes of PWL) of 50 mg/kg cannabinoids i.p. in CFA-induced inflammatory pain (linear regression, $n = 11$). (B and C) The K_i values of cannabinoid binding affinity for CB1 receptors (B) or CB2 receptors (C) versus the analgesic potency of cannabinoids. (D–F) Cannabinoid (1 μM)-induced potentiation of I_{Gly} versus the effects of 50 mg/kg cannabinoids i.p. on body temperature (D), locomotor activity (E), or rotarod performance (F). (G–I) The analgesic potency of 50 mg/kg cannabinoids i.p. versus the effect of cannabinoids on body temperature (G), locomotor activity (H), or rotarod performance (I). Data are representative of two to three independent experiments.

interaction, provide only limited information about direct binding at the site involving S296. To address these issues, we first converted the $\alpha 1$ subunit to the $\alpha 3$ subunit by mutating all 12 residues to match the $\alpha 3$ sequence. Using the high-resolution NMR structure of $\alpha 1$ GlyR TM domains solved in the lyso-1-palmitoylphosphatidylglycerol (LPPG) lipids as a template, we generated a homology model of $\alpha 3$ GlyR-TM structure (Fig. 8 A). We next measured the interaction between CBD and $\alpha 3$ GlyR TM domains by chemical shift titration using two-dimensional (2D) ^{15}N heteronuclear single quantum coherence (HSQC) spectroscopy and by 3D ^{15}N -edited nuclear Overhauser effect spectroscopy (NOESY) as well as 2D homonuclear ^1H - ^1H NOESY. HSQC spectroscopy revealed that S296 in the TM3 domain was distinctively sensitive to CBD titration. Representative contour plots of the S296 HSQC resonance at different CBD concentrations are depicted in Fig. 8 B. With increasing CBD concentrations, the S296 resonance exhibited CBD-dependent changes both in chemical shift and in intensity. It is worth noting that at an intermediate CBD concentration (105 μM), S296 resonance became two distinct peaks, suggesting two coexisting states of binding on a relatively slow exchange time scale or two

different protein conformations at S296. As CBD concentration continued to increase, the binding or conformational state corresponding to the downfield resonance (Fig. 8 B, left peak) became dominant.

To determine whether or not CBD can directly interact with $\alpha 3$ GlyR-TM, we examined the intermolecular NOESY cross peaks between CBD and the protein. Fig. 8 C compares the contour plots of NOESY cross peaks between the aromatic protons of CBD (~ 6.2 – 6.4 ppm) and other proton resonances in the 1–4 ppm range in the absence and presence of $\alpha 3$ GlyR-TM, respectively. In the absence of the protein, intramolecular cross peaks of CBD in LPPG can be detected at ~ 1.3 , 1.6, and 2.5 ppm (Fig. 8 C). In the presence of $\alpha 3$ GlyR-TM, an additional cross peak was observed at ~ 3.9 ppm. This resonance was assigned to $\text{H}\beta$ of S296. The presence of an intermolecular cross peak is a strong indication that CBD interacts with the TM domain of $\alpha 3$ GlyR subunit specifically at a site involving S296. The transition from the free to the CBD-bound state seems to induce a conformational change in the protein at S296, as can be clearly seen from the gradual disappearance of the free S296 resonance and appearance of the bound

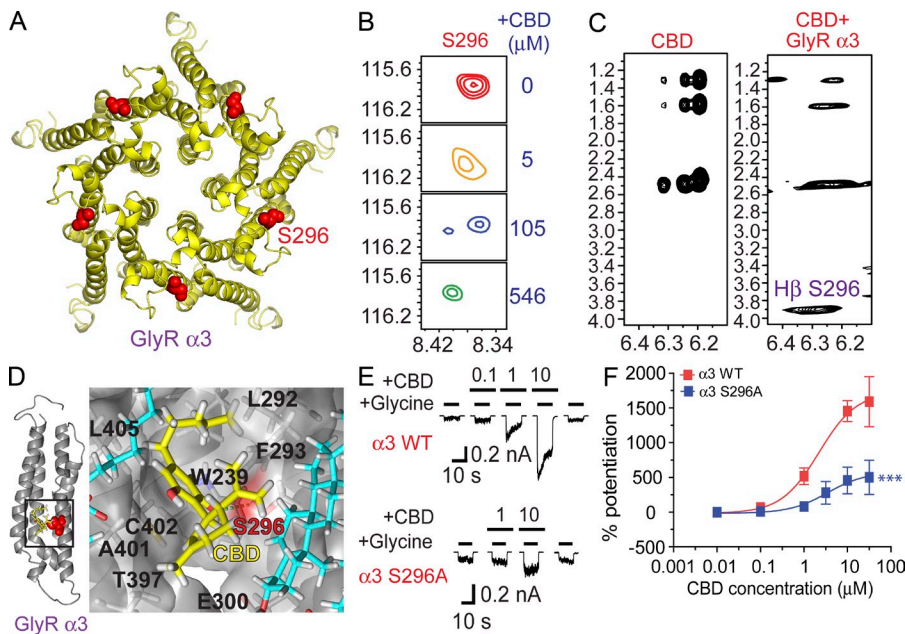


Figure 8. NMR analysis: a direct inter-action between CBD and S296-containing domain of $\alpha 3$ GlyR.

(A) A homology model of $\alpha 3$ GlyR-TM domain structure derived from the high-resolution NMR structure of $\alpha 1$ GlyR TM domains. S296 residue is highlighted in red. (B) Contour plots of the S296 resonance in the HSQC spectrum of the $\alpha 3$ GlyR TM domains in LPPG micelles as a function of CBD concentrations: red, 0 μM ; orange, 5 μM ; blue, 105 μM ; and green, 546 μM . (C) Strip plots of the 2D ^1H - ^1H NOESY spectra in the absence and presence of $\alpha 3$ GlyR TM domains, showing an unambiguous cross peak between the aromatic protons of CBD and the $\text{H}\beta$ of S296. (D) Side views of a proposed binding interaction between CBD and the $\alpha 3$ GlyR-TM involving the S296, as revealed by a molecular dynamic simulation of 20 ns. The S296 residue is indicated in red and CBD is indicated in yellow. Lipids surrounding the S296-containing domain are indicated in blue. (E) Traces of CBD-induced potentiation on I_{Gly} in HEK 293 cells expressing the WT ($n = 5$) and mutant S296A ($n = 6$) $\alpha 3$ GlyRs. (F) The concentration-response curves of CBD-induced potentiation of the $\alpha 3$ GlyRs. ***, $P < 0.001$ (WT vs. S296A). Data are representative of two independent experiments and expressed as mean \pm SEM.

resonance, with an intermediate coexistence of both peaks (Fig. 8 B). NMR titration and NOESY experiments suggest a direct interaction of CBD with residue S296. Based on this idea, we performed several parallel molecular dynamics simulations of 20 ns each with different random seeds to determine the molecular nature of the interaction between CBD and the binding site involving S296. Fig. 8 D depicts a typical frame from simulation trajectories showing details of the binding pocket for CBD. DD-CBD inhibited DH-CBD-induced potentiation of I_{Gly} in an apparent competitive manner, as revealed by our electrophysiological experiments. In this regard, we next compared the docking free energies between CBD and DD-CBD at the S296 site and found that binding affinities of CBD and DD-CBD are within the same order of magnitude with similar docking free energies (unpublished data). This finding favors the idea that DD-CBD inhibition of CBD potentiation of I_{Gly} is through a competitive mechanism by acting near or at the same site involving S296. Consistent with our NMR and MD simulation that CBD interacts with $\alpha 3$ GlyR at S296, substitution of S296 with an alanine in the $\alpha 3$ GlyR significantly reduced the magnitude of CBD potentiation by nearly 70% (Fig. 8, E and F).

Besides S296, residue T397 in the loop leading to the fourth transmembrane domain (TM4) of $\alpha 3$ GlyR was also affected by the CBD titration (unpublished data). T397 is evidently in an intrinsically dynamic region of the protein, showing two conformations with an exchange rate slower than the NMR time scale (and hence two distinct HSQC resonances for T397) even in the absence of CBD. Binding of CBD at S296 also altered the motional characteristics of T397, resulting in the disappearance of one of the conformations at T397. We could not determine the functional role of the residue T397 in

CBD-induced potentiation because the T397A mutation resulted in low expressions of the $\alpha 3$ GlyRs in HEK 293 cells.

Kinetic analysis: DH-CBD accelerates GlyR activation rate and slows deactivation rate

The observations mentioned in the previous section suggest that CBD directly interacts with S296-containing domain in the $\alpha 3$ GlyR protein. To further explore mechanistic detail of the interaction between cannabinoids and GlyRs, we examined the effect of DH-CBD on GlyR kinetics using fast drug perfusion in HEK-293 cells expressing $\alpha 3$ GlyRs. DH-CBD at 3 μM accelerated the initial slope of the activation phase of the current activated by 1 mM glycine (Fig. 9 A). The 10–90% activation times were 11.1 ± 0.8 and 5.8 ± 0.8 ms in the absence and presence of 3 μM DH-CBD, respectively. These values were significantly different ($P < 0.05$). The S296A mutation and DD-CBD pretreatment completely abolished DH-CBD-induced acceleration of receptor activation time (11.3 ± 0.7 vs. 11.4 ± 0.4 ms for S296A and 10.5 ± 1.3 vs. 10.8 ± 1.3 ms for DD-CBD, $P = 0.4$ – 0.6). DH-CBD significantly slowed the receptor deactivation time constant from 10.9 ± 0.5 to 41.3 ± 4.8 ms immediately after a 5-ms application of 1 mM glycine (Fig. 9 B, $P < 0.001$). The S296A mutation and DD-CBD prevented DH-CBD-induced alteration of receptor deactivation time (11 ± 1.7 vs. 14.2 ± 3.7 ms for S296 and 11.7 ± 0.8 vs. 16.6 ± 3.3 ms for DD-CBD, $P > 0.05$). In contrast, DH-CBD did not significantly alter receptor desensitization time (3.4 ± 0.2 vs. 3.8 ± 0.4 s, $P > 0.05$). These observations suggest that DH-CBD may increase agonist

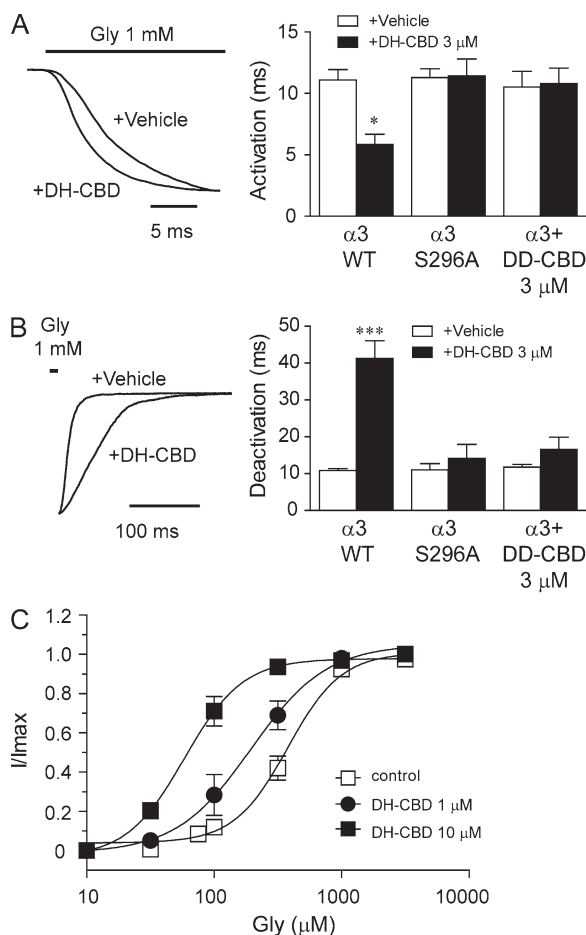


Figure 9. The effect of DH-CBD on α 3 GlyR gating kinetics and agonist affinity. (A) Traces of currents activated by 1 mM glycine in HEK 293 cells expressing WT or S296A mutant α 3 GlyRs in the absence and presence of 3 μ M DH-CBD. Bar graph shows the mean activation time constant ($n = 6-9$). Asterisks indicate a significant difference as compared with vehicle (*, $P < 0.05$). (B) Traces of currents during a washout after a 10-ms application of 1 mM glycine in the absence and presence of 3 μ M DH-CBD. The bar graph shows mean deactivation time constants ($n = 6-7$). The asterisk indicates a significant difference as compared with vehicle (***, $P < 0.001$). (C) The glycine concentration-response curves in the absence ($n = 6$) and presence of 1 μ M ($n = 8$) and 10 μ M ($n = 5$) DH-CBD. Data are representative of two independent experiments and expressed as mean \pm SEM.

binding affinity. Consistent with this idea, DH-CBD caused a parallel leftward shift in the glycine concentration-response curve (Fig. 9 C). The EC_{50} values of glycine were reduced from 377 ± 45 to 195 ± 51 and 58 ± 13 μ M in the absence and presence of 1 and 10 μ M DH-CBD in HEK 293 cells expressing α 3 GlyRs. These values were significantly different ($P < 0.05$).

DISCUSSION

Spinal α 3 GlyRs have been proposed as an important target for pain treatment. However, the α 3 GlyR-based therapeutic agents in the treatment of chronic pain or other diseases are

not yet available. The current study has provided several lines of evidence to suggest that CBD and DH-CBD suppress persistent inflammatory and neuropathic pain by targeting the α 3 GlyRs in rodents. Consistent with in vitro observation that DH-CBD was more efficacious than CBD in potentiating I_{Gly} , DH-CBD was more potent than CBD in reducing chronic pain. DH-CBD also attenuated i.t. PGE_2 -induced persistent pain hypersensitivity in mice. Several lines of evidence suggest that cannabinoid-induced analgesia is mediated through the α 3 GlyR-dependent pathway. First, both CBD and DH-CBD-induced analgesic effects were significantly reduced in mice lacking the α 3 GlyRs but not in mice lacking the CB1 and CB2 receptors. Second, DD-CBD inhibited DH-CBD-induced potentiation of the α 3 GlyRs and analgesic effect in chronic pain. Third, structural and functional analysis reveals that the magnitude of the cannabinoid-induced analgesic effect was correlated with cannabinoid potentiation of the α 3 GlyRs but not with cannabinoid binding affinity for CB1 and CB2 receptors. Because of substantially reduced CB1 binding affinity, DH-CBD, even at high concentrations (50 mg/kg i.p.), did not produce the psychoactive effects commonly associated with cannabinoid activation of CB1 receptors. Collectively, glycinergic cannabinoids represent a new class of therapeutic agents that selectively relieve pathological pain by targeting the α 3 GlyRs.

The data from NMR titration and NOESY experiments strongly indicates the direct interaction of CBD with residue S296. The change in NMR signal intensity upon CBD titration suggests that the protein motion at S296 is sensitive to CBD binding. The molecular model of the α 3 GlyR TM domains reveals that S296 is located near the intracellular end of the TM3 helix, with its side chain facing the lipids. Direct interaction of CBD with α 3 GlyR-TM protein was confirmed by the intermolecular NOESY cross peaks between CBD and the protein. There is a transition from the free to the CBD-bound state as indicated by the observation that a free S296 resonance and a bound resonance appeared sequentially with an intermediate coexistence of both peaks. This finding also favors a protein conformational change at S296 in the presence of CBD.

Our molecular dynamics simulations suggest that CBD- α 3 GlyR binding interactions involve the S296 residue of the α 3 GlyR TM domain on the principal side, and the lipid molecules on the complementary side. The molecular docking analyses reveal that the binding free energies of the potentiator CBD and the inhibitor DD-CBD at this protein-lipid interfacial site are very similar, suggesting that the binding affinities are within the same order of magnitude. This finding favors the idea that the DD-CBD inhibition of CBD potentiation of I_{Gly} is through a competitive mechanism by acting near or at the same site involving S296. It should be pointed out that both DH-CBD and DD-CBD are modulators of GlyRs. Unlike orthosteric ligands, these modulators bind to allosteric sites. The molecular nature of competitiveness of these modulators remains unknown. Although the data from the in vitro study together with the result of molecular dynamics

simulations suggest that DD-CBD may compete for the same site with CBD, our experimental data alone are not sufficient to conclude that DD-CBD acts as a competitive antagonist of CBD. Future studies should be performed to examine the effect of DD-CBD on the purified $\alpha 1$ or $\alpha 3$ GlyR-TM proteins using NMR analysis.

The kinetic analysis suggests that DH-CBD increases the agonist binding affinity of GlyRs. DH-CBD accelerated receptor activation rate and, on the other side, slowed receptor deactivation rate. Although receptor activation time represents agonist binding and/or channel gating, receptor deactivation time reflects the kinetics of agonist unbinding/channel closing or combination of two. The DH-CBD-induced changes in GlyR kinetics appears relevant to DH-CBD-induced potentiation of I_{Gly} because both S296A and DD-CBD, which inhibited DH-CBD potentiation of I_{Gly} , abolished DH-CBD alteration of receptor gating kinetics. DH-CBD shifted in a parallel manner the glycine-concentration response curve to the left, favoring a hypothesis that DH-CBD allosterically increases the agonist binding affinity of GlyRs. However, this notion should be made with caution, as slow deactivation time of GlyRs could reflect a slow channel closing, unbinding rate, or both in the presence of DH-CBD. In this scenario, slow deactivation time could be a result of slow wash time of DH-CBD because of its hydrophobic nature. One can also argue that the deactivation rate could be contaminated with desensitization rate. However, it is unlikely to be the case in our study because DH-CBD did not significantly affect GlyR desensitization rate while slowing deactivation.

Several preclinical persistent and chronic pain models were tested in this study. Intraplantar CFA injection has been widely used as an inflammatory pain model. Both systemic and i.t. injection of DH-CBD significantly reduced mechanical pain hypersensitivity induced by CFA. PGE₂ is one of the major proinflammatory substances that promote nociceptive processing in the spinal cord and peripheral tissues upon various noxious stimuli such as CFA (Vanegas and Schaible, 2001; Harvey et al., 2004, 2009; Zeilhofer et al., 2012). Consistent with the observations in CFA-induced inflammatory pain models, DH-CBD also produced an analgesic effect in i.t. injection of PGE₂-induced nociception in mice. More importantly, i.t. application of DH-CBD exerted potent inhibition of chronic neuropathic pain in rats. Neuropathic pain is a substantial health issue because currently available therapies are far from satisfactory. Although neuropathic pain and inflammatory pain differ in pathogenesis, molecular mechanisms, and treatments, these two types of persistent pain may be modulated by similar synaptic mechanism at the spinal level (Zeilhofer et al., 2012). The data presented in our study suggest that the $\alpha 3$ GlyR contributes to the mechanisms that modulate both types of pain. Yet, we cannot exclude the potential involvement of other subtypes of GlyRs in the pain modulation. In addition to reducing chronic pain, DH-CBD can also attenuate acute pain. DH-CBD increased the time latency in the tail flick reflex in mice (Xiong et al., 2011). This analgesic effect induced by DH-CBD was abolished

in mice depleted with the $\alpha 3$ GlyRs but remained intact in mice depleted with the CB1 receptors. Consistent with this idea, i.t. application of DH-CBD at higher doses also significantly increased the contralateral PWL from baseline in both inflammatory and neuropathic pain in rats.

i.t. application of DH-CBD seems the most efficacious way to suppress mechanical and thermal pain hypersensitivity in both inflammatory and neuropathic pain conditions. This idea is consistent with the distinct distribution pattern of the $\alpha 3$ GlyRs in lamina II of the spinal dorsal horn (Harvey et al., 2004). Moreover, the $\alpha 3$ GlyRs are either absent or less expressed in primary sensory neurons such as dorsal root ganglion neurons (Lynch, 2004). Oral administration of cannabinoids is not an ideal route for drug delivery because primary cannabinoids are largely metabolized by the liver (Huestis and Pertwee, 2005). It is worth mentioning that one of the common practices to deliver medical cannabis to humans is via sublingual spray, which bypasses the liver and delivers drugs directly into the blood stream (Nurmikko et al., 2007). Collectively, we propose that i.t. injection of cannabinoids should be the most efficacious route to treat patients with chronic neuropathic pain.

Among 11 cannabinoid analogues evaluated in this study, DH-CBD has emerged as an ideal glycinergic cannabinoid that can be used to treat chronic pain without causing aversive effects. Unlike some of the analogues that not only showed relatively high efficacy in potentiating I_{Gly} but also demonstrated relatively high affinity to bind to CB1 receptors, DH-CBD displayed a low affinity for CB1 receptors and at the same time is one of the most efficacious positive modulators of GlyRs. It has been shown consistently in our correlation analysis that most psychoactive effects induced by cannabinoids are associated with CB1 receptor binding affinity but not cannabinoid-induced potentiation of GlyRs. Conversely, the cannabinoid-induced analgesic effect in chronic pain is correlated with cannabinoid potentiation of GlyRs but not with cannabinoid binding affinity to CB1 receptors. These principles may apply to future studies in developing a new generation of glycinergic cannabinoids in the treatment of chronic pain. In addition to lacking a psychoactive side effect, glycinergic cannabinoids are unlikely to develop drug tachyphylaxis or tolerance, one of the major barriers for long-term pain management with currently available clinical agents. Repeated application of DH-CBD either i.p. or i.t. exhibited similar analgesic potency in both inflammatory and neuropathic pain. This finding is not unexpected because glycinergic cannabinoids act on the GlyRs as allosteric modulators instead of agonists or antagonists.

Collectively, we have provided evidence to suggest that glycinergic cannabinoids are ideal therapeutic agents in the treatment of inflammatory and neuropathic pain. They can effectively attenuate pathological pain without significantly causing major psychoactive side effect and analgesic tolerance. The mechanistic details of drug-receptor interaction could help to develop novel agents for the treatment of painful conditions and other diseases involving GlyR impairment.

MATERIALS AND METHODS

Animals. All behavioral experiments were conducted in male C57BL/6J mice unless otherwise indicated. All animal studies were performed under the protocols proved by Animal Care and Use Committees of University of Maryland, the Johns Hopkins University, the University of Texas MD Anderson Cancer Center, and the National Institute on Alcohol Abuse and Alcoholism. Adult C57BL/6J male mice were purchased from The Jackson Laboratory at the age of 8 wk. The $\alpha 3$ Glra mice were purchased from The Jackson Laboratory. The $\alpha 3$ Glra^{+/-} mice were bred with each other to generate experimental animals: WT, $\alpha 3$ Glra^{+/-}, and $\alpha 3$ Glra^{-/-} littermates. The CB1^{-/-} and CB2^{-/-} mice were generated as previously described (Zimmer et al., 1999; Buckley et al., 2000). The homozygous mutants of these mice were backcrossed into the C57BL/6J background for at least six generations. Genotyping of the $\alpha 3$ Glra mutant mice was done using the following primers: forward primer KO, 5'-GACGAGTCTTCTGAGGGGATCGATC-3'; forward primer WT, 5'-ACTGCTCATAGGCTGGTGTGATATG-3'; and reverse primer WT/KO, 5'-GAGGAAACTTTGCAGTCCTT-ACCTG-3'. Genotyping of the CB1 mutant mice was done using the following primers: forward primer (CB1F), 5'-GTACCATCACCA-CAGACCTCTC-3'; reverse primer KO (CNKO3), 5'-AAGAAC-GAGATCAGCAGCCTCTGTT-3'; and reverse primer WT (CB1wt), 5'-GGATTGAGAATCATGAAGCACTCCA-3'. Genotyping of the CB2 mutant mice was done using the following primers: forward primer (CB2 P1), 5'-AAATGCTTGATTGGTGTGTCAGCTCTC-3'; reverse primer KO (CB2 P3), 5'-TAAAGCGCATGCTCCAGACTGCCTT-3'; and reverse primer WT (CB2wt P2), 5'-GGCTCCTAGGTGGTTTTCATCAGCCTCT-3'. All pain behavioral testing was conducted by a blinded observer.

Inflammatory pain model in mice. Inflammation was induced with intraplantar injection of 10 μ l CFA (diluted 1:4 with saline; Sigma-Aldrich) to the left hind paw. The PWL to noxious heat was measured using a system described previously (Bai et al., 2010). The injected hind paw showed edema and erythema indicating inflammation (Bai et al., 2010).

Neuropathic pain model in rats. The L5 spinal nerve of adult, male Sprague-Dawley rats (300–350 g; Harlan Bioproducts for Science) was ligated as described previously (Guan et al., 2008). The animals were anesthetized with isoflurane (2%; Abbott Laboratories). The left L5 spinal nerve was tightly ligated with a 6–0 silk suture and cut distally. The muscle layer was closed with 4–0 silk suture and the skin closed with metal clips.

Inflammatory pain model in rats. Inflammation was induced with CFA suspended in an oil/saline 1:1 emulsion and 0.1 mg was injected s.c. (Mycobacterium) into the plantar surface of the left hind paw. The injection produced intense tissue inflammation of the hind paw characterized by erythema, edema, and hyperalgesia that were confined to the injected hind paw.

i.t. injection in mice. i.t. drug injection was performed as described by Hylden and Wilcox (1980) with a few modifications. To avoid possible stress induced during i.t. injection, mice were anesthetized with isoflurane (2%) during injection. A 30-gauge steel-tip needle connected with a 50- μ l syringe was used for the injection. Mice usually recovered within 2–3 min after the injection. The volume of the injection was 5 μ l and saline was used as a control. Drugs were always prepared freshly on the day of experiments and dissolved in saline.

i.t. catheter implantation and injection in rats. The atlanto-occipital membrane at the level between the head and neck was exposed, and a small slit was cut, into which a 6–7-cm length of saline-filled PE-10 tubing was inserted. The animals were allowed to recover for 4–5 d before testing. After completion of the experiment, we confirmed i.t. drug delivery by injecting 400 μ g/20 μ l lidocaine (Hospira) through the catheter. When the catheter was properly placed, the lidocaine induced a temporary motor paralysis and sensory block of the lower limbs (Dobos et al., 2003). To avoid causing

stress, drugs were administered to animals i.t. under brief inhalation anesthesia (1.5% isoflurane for 1–2 min). A drug solution was slowly infused in a volume of 15 μ l, followed by flushing the catheter with 10 μ l saline.

Pain measurement in rats. Hypersensitivity to punctuate mechanical stimulation in rats was determined with the up-down method using a series of von Frey filaments (0.38, 0.57, 1.23, 1.83, 3.66, 5.93, 9.13, and 13.1 g) as described previously (Chaplan et al., 1994). The von Frey filaments were applied for 4–6 s to the test area between the footpads on the plantar surface of the hind paw. If a positive response occurred (e.g., abrupt paw withdrawal, licking, and shaking), the next smaller von Frey hair was used; if a negative response was observed, the next higher force was used. The test was continued until: (1) the responses to five stimuli were assessed after the first crossing of the withdrawal threshold or (2) the upper/lower end of the von Frey hair set was reached before a positive/negative response had been obtained. The PWT was determined according to the formula provided by Dixon (1980).

Measurement of thermal pain hypersensitivity in mice and rats.

Thermal pain hypersensitivity was determined by measuring PWL to radiant heat stimuli (Hargreaves et al., 1988) with a plantar stimulator analgesia meter (model 390; IITC). Animals were placed under individual plastic boxes on a heated glass floor (30°C) and allowed to habituate for at least 30 min before testing. Both hind paws were tested three times, with >2 min between trials. A cut-off time of 20 s was used to avoid sensitization and damage to the skin. The mean PWL of the three trials was used for data analysis.

Measurement of body temperature. Mouse body temperature was measured by inserting a thermometer (Thermalert TH-5; Physitemp) 2 cm into the rectum until a stable reading was obtained. Ambient room temperature was 22°C.

Locomotor activity. Mice were i.p. injected with the vehicle or cannabinoids. After 15 min, the spontaneous locomotor activity of mice was measured in a standard home cage in a 12-station photobeam activity system (Opto-M3 Activity Meter; Columbus Instruments) where the animals were placed individually 30 min after injection of drugs. Using infrared beams, activity was monitored in the horizontal directions. The total number of ambulatory beam breaks was recorded for 30 min and stored every 10 s.

Rotarod test. A computer-interfaced rotarod accelerating from 4–40 rotations per min over 300 s was used (ENV-575M; Med Associates). The shaft diameter is 3.2 cm. The mice were trained three trials per day with a 20-min interval for three consecutive days. Each trial ended when the mouse fell off the rotarod or after 300 s had elapsed. The time that each mouse maintained its balance on the rotating rod was measured as latency to fall.

HEK 293 cell transfection and recording. HEK 293 cells were cultured as described previously (Xiong et al., 2008). The plasmid cDNAs of the WT and mutant GlyR subunits and EP2R were transfected using the SuperFect Transfection kit (QIAGEN). The currents were recorded 1–2 d after transfection. HEK 293 cells, but not neurons, were lifted and continuously superfused with a solution containing 140 mM NaCl, 5 mM KCl, 1.8 mM CaCl₂, 1.2 mM MgCl₂, 5 mM glucose, and 10 mM Hepes (pH 7.4 with NaOH; ~340 mOsmol with sucrose). Membrane currents were recorded in the whole-cell configuration using an amplifier (Axopatch 200B; Axon) at 20–22°C. Cells were held at –60 mV unless otherwise indicated. Data were acquired using pClamp 9.2 software (Molecular Devices). Data were filtered at 1 KHz and digitized at 2 KHz. Bath solutions were applied through three barrel square glass tubing (Warner Instrument) with a tip diameter of ~200 μ m. Drugs were applied through a Warner fast-step stepper-motor driven system. The solution exchange time constants were ~4 ms for an open pipette tip and 4–12 ms for whole-cell recording.

Site-directed mutagenesis. Point mutations of the rat $\alpha 3$ GlyR were introduced using a QuikChange Site-Directed Mutagenesis kit (Agilent Technologies). The authenticity of the DNA sequence through the mutation sites

was confirmed by double-stranded DNA sequencing using a CEQ 8000 Genetic Analysis System (Beckman Coulter).

Spinal cord slice preparation and electrophysiological recordings.

Lumbar spinal cord slices at the L5-L6 level were prepared from adult rats as we described previously (Pan and Pan, 2004; Zhou et al., 2008). We removed the lumbar spinal cord through laminectomy during isoflurane-induced anesthesia. We sliced the spinal cord (400 μm) using a vibratome and continually superfused the slices with artificial cerebrospinal fluid containing (in mM) 117.0 NaCl, 3.6 KCl, 1.2 MgCl_2 , 2.5 CaCl_2 , 1.2 NaH_2PO_4 , 11.0 glucose, and 25.0 NaHCO_3 (bubbled with 95% O_2 /5% CO_2). Neurons in the lamina II of the spinal cord were visualized using a fixed-stage microscope (BX50WI; Olympus) with differential interference contrast/infrared illumination. We obtained all whole-cell patch-clamp recordings at 34°C using glass pipettes filled with a solution containing (in mM) 110 Cs_2SO_4 , 5 TEA, 2.0 MgCl_2 , 0.5 CaCl_2 , 5.0 Hepes, 5.0 EGTA, 5.0 ATP-Mg, 0.5 Na-GTP, and 10 lidocaine *N*-ethyl bromide, adjusted to pH 7.2–7.4 with 1 M CsOH (290–300 mOsm). GlyR-mediated currents were recorded at the holding potential of 0 mV and elicited by puff application of 30 μM glycine directly to the recorded neuron using a positive pressure system (4 psi for 15 ms; Toohey Company). The input resistance was continuously monitored, and the recording was abandoned if it changed >15%. Data acquisition and analysis of postsynaptic currents were done as described previously (Pan and Pan, 2004; Zhou et al., 2008).

[^3H]-CP55940 binding of CB1 and CB2 receptors. Mouse brain tissues (CB1) and Rosetta(DE3) pLysS competent *E. coli* cells (EMD) transfected with human CB2 receptor cDNA were collected and homogenized using a polytron homogenizer (Brinkman) at 500 rpm for 30 s in ice-cold 50 mM Tris-HCl, 1 mM EDTA, and 3 mM MgCl_2 , pH 7.4. The homogenate was centrifuged at 48,000 g for 20 min at 4°C. The membrane pellet was suspended and incubated with [^3H]-CP55940 (PerkinElmer) and various concentrations of cannabinoids in phosphate buffered saline (PBS) containing 0.2% (wt/vol) BSA at 30°C for 60 min. Nonspecific binding was determined in the presence of 10 μM of CP55940. Bound and free [^3H]-CP55940 was separated by rapid vacuum filtration in a Brandell harvester through GF/B filters. The filters were washed four times with 4 ml cold PBS containing 0.1% (wt/vol) BSA. The filters were punched into scintillation vials containing 5 ml liquid scintillation cocktail. The samples were counted in a scintillation counter at 50% efficiency. Assays were performed in triplicate, and each experiment was repeated at least three times.

NMR spectroscopy. Interaction between CBD and the transmembrane (TM) domain of the human GlyR $\alpha 3$ subunit ($\alpha 3$ GlyR-TM) was investigated by NMR spectroscopy. The full-length $\alpha 3$ GlyR TM domains have a sequence of MLERQLGYLL IQLYIPSLI VILSWVFWI NLDAAPARVALGITTVLTLT TQSSGSRASL PKVSYVKAID IWLAVCLLFV FSALLEYAAV NFVSRQHKEG GGGFIDRAKK IDTISRACFP LAFLIFNIFY WVYIKILRRE DEFHHHHHHH. The DNA plasmid for protein expression was prepared by mutating all 12 amino acid residues in the $\alpha 1$ GlyR-TM plasmid to match those in the $\alpha 3$ sequence (Ma et al., 2005; Canlas et al., 2008; Xiong et al., 2011). The large intracellular loop between TM3 and TM4 domains was replaced with a glycine linker (GGGG). The same expression and purification protocols used for $\alpha 1$ GlyR-TM (Ma et al., 2005; Canlas et al., 2008; Xiong et al., 2011) were followed. The NMR samples typically contained 100 μM $\alpha 3$ GlyR-TM solubilized in ~ 15 mM of LPPG in 10 mM sodium phosphate buffer, pH 5.8. 2D ^{15}N HSQC spectroscopy and 3D ^{15}N -edited NOESY, as well as 2D ^1H - ^1H NOESY, were recorded on Avance 600 and 800 MHz spectrometers (Bruker) at 313 K, with a complex time-domain size of $1,024 \times 128$, $1,024 \times 32 \times 88$, and $1,024 \times 370$, respectively. NOESY mixing time was 120 ms. NMR chemical shift titration experiments were performed at CBD concentrations of 0, 5, 105, and 546 μM . The NMRPipe (Delaglio et al., 1995) and Topspin programs were used for NMR data processing, and the Sparky program (SPARKY 3; T.D. Goddard and D.G. Kneller, University of California, San Francisco, San Francisco, CA) was used for analyzing the spectra and for preparing the figures.

Molecular dynamics simulations. The structure of $\alpha 3$ GlyR-TM was generated from the NMR structure of $\alpha 1$ GlyR-TM using MODELLER 9v8 (Eswar et al., 2007) and manually inserted into a fully hydrated ternary lipid mixture as detailed previously (Cheng et al., 2007). The force-field parameters for CBD were generated using CHARMM general force field (Vanommeslaeghe et al., 2010) with high penalties further optimized using Gaussian 09 (Gaussian, Inc.) at the MP2/6-31G(d) level (Møller and Plesset, 1934) and tested using CHARMM c36b1 (Liu et al., 2004; Saladino and Tang, 2004; Brooks et al., 2009). All simulations were performed using NAMD 2.7b1 (Phillips et al., 2005). Guided by the experimental NMR data, the initial CBD location near S296 was determined by docking, followed by production molecular dynamics simulations in replica lasting 20 ns each. The final simulation frames were used to analyze the binding site for CBD in $\alpha 3$ GlyR-TM. The binding site was used in AutoDock 4.0 (Morris et al., 1998) to evaluate interaction between DD-CBD and $\alpha 3$ GlyR-TM. For both CBD and DD-CBD, docking results were compiled from separate 300 runs using the Lamarckian genetic algorithm implemented in AutoDock 4.0. In each case, a population size of 300, a maximum of 27,000 generations, and a maximum of 15 million energy evaluations were used.

Whole-cell kinetic measurements. Receptor activation rate for current induced by 1 mM glycine was estimated by measuring the slope of the initial inward component of current between 10 and 90% of the maximal current (10–90% rise time). Receptor desensitization was induced by 1 mM glycine for 10 s in cells voltage-clamped at -60 mV. The deactivation time was recorded for 30 s immediately after 10 ms application of 1 mM glycine. The time constants of deactivation and desensitization were determined by fitting with mono-exponential functions using the Levenberg-Marquardt algorithm in Clampfit 9.2 (Molecular Devices).

Drugs. Most of the chemicals including glycine were from Sigma-Aldrich. Solutions were prepared on the day of experiment. THC was obtained from the National Institute on Drug Abuse. HU210 and CP55940 were obtained from Tocris Bioscience. Agonists and other chemical agents were diluted either directly in the bath solution or dissolved in ethanol before further dilution. The final ethanol concentration was <8 mM, which did not significantly affect I_{Gly} . DD-CBD was originally dissolved in DMSO in a stock solution and further diluted in working solution (external buffer). The maximal concentration of DMSO in bath solution was <0.1%. This concentration of DMSO alone did not affect I_{Gly} . In behavioral tests, all drugs were dissolved in drug/emulphor/saline solution with a ratio of 1:1:18. Emulphor was obtained from North American Chemical. The vehicles used in our experiments did not affect latency responses when administered alone.

Data analysis. Statistical analysis of concentration–response data were performed with the use of the nonlinear curve-fitting program Prism (Graph-Pad Software). Data were fit using the Hill equation $I/I_{\text{max}} = \text{Bottom} + (\text{Top} - \text{Bottom}) / (1 + 10^{(\text{LogEC}_{50} - \text{Log}[\text{Agonist}]) \times \text{HillSlope}})$, where I is the current amplitude activated by a given concentration of agonist, I_{max} is the maximum response of the cell, and EC_{50} is the concentration eliciting a half-maximal response.

A one-way repeated measures ANOVA was used to compare the data between time points in each group. Data from different drug groups were compared using a two-way mixed model ANOVA. The Tukey's honestly significant difference post-hoc test was used to compare specific data points in ANOVA. STATISTICA 6.0 software (StatSoft, Inc.) was used for analysis, and data are expressed as mean \pm SEM. $P < 0.05$ was considered significant.

Online supplemental material. Figure S1 lists the names and chemical structures of 11 synthetic cannabinoids structurally similar to CBD. Figure S2 shows the procedures of chemical synthesis of cannabinoid analogues. Online supplemental material is available at <http://www.jem.org/cgi/content/full/jem.20120242/DC1>.

We thank Dr. Pei Tang for help with NMR data analyses and molecular dynamics simulations. We thank Drs. Alex Yelinev and Zhifeng Zhou for providing purified CB₂ receptor protein and DNA sequencing. We thank Mr. Dong Wei for technical assistance with animal studies. We thank Dr. David M. Lovinger for critical comments on the manuscript. We thank Drs. David M. Lovinger and Kenner Rice for instrument support.

This work was supported by funds from the intramural program of the National Institute on Alcohol Abuse and Alcoholism, and grants R01-NS070814-01 (to Y. Guan), NS073935 (to H.L. Pan), and T32GM075770 and R37GM049202 (to Y. Xu) from the National Institutes of Health.

The authors declare that they have no competing financial interests.

Submitted: 31 January 2012

Accepted: 23 April 2012

REFERENCES

- Ahmadi, S., S. Lippross, W.L. Neuhuber, and H.U. Zeilhofer. 2002. PGE(2) selectively blocks inhibitory glycinergic neurotransmission onto rat superficial dorsal horn neurons. *Nat. Neurosci.* 5:34–40. <http://dx.doi.org/10.1038/nm778>
- Ahrens, J., R. Demir, M. Leuwer, J. de la Roche, K. Krampfl, N. Foadi, M. Karst, and G. Haeseler. 2009a. The nonpsychotropic cannabinoid cannabidiol modulates and directly activates alpha-1 and alpha-1-Beta glycine receptor function. *Pharmacology.* 83:217–222. <http://dx.doi.org/10.1159/000201556>
- Ahrens, J., M. Leuwer, R. Demir, K. Krampfl, J. de la Roche, N. Foadi, M. Karst, and G. Haeseler. 2009b. Positive allosteric modulatory effects of ajulemic acid at strychnine-sensitive glycine alpha1- and alpha1beta-receptors. *Naunyn Schmiedebergs Arch. Pharmacol.* 379:371–378. <http://dx.doi.org/10.1007/s00210-008-0366-8>
- Bai, G., D. Wei, S. Zou, K. Ren, and R. Dubner. 2010. Inhibition of class II histone deacetylases in the spinal cord attenuates inflammatory hyperalgesia. *Mol. Pain.* 6:51. <http://dx.doi.org/10.1186/1744-8069-6-51>
- Brooks, B.R., C.L. Brooks III, A.D. Mackerell Jr., L. Nilsson, R.J. Petrella, B. Roux, Y. Won, G. Archontis, C. Bartels, S. Boresch, et al. 2009. CHARMM: the biomolecular simulation program. *J. Comput. Chem.* 30:1545–1614. <http://dx.doi.org/10.1002/jcc.21287>
- Buckley, N.E., K.L. McCoy, E. Mezey, T. Bonner, A. Zimmer, C.C. Felder, M. Glass, and A. Zimmer. 2000. Immunomodulation by cannabinoids is absent in mice deficient for the cannabinoid CB(2) receptor. *Eur. J. Pharmacol.* 396:141–149. [http://dx.doi.org/10.1016/S0014-2999\(00\)00211-9](http://dx.doi.org/10.1016/S0014-2999(00)00211-9)
- Burns, T.L., and J.R. Ineck. 2006. Cannabinoid analgesia as a potential new therapeutic option in the treatment of chronic pain. *Ann. Pharmacother.* 40:251–260. <http://dx.doi.org/10.1345/aph.1G217>
- Canlas, C.G., D. Ma, P. Tang, and Y. Xu. 2008. Residual dipolar coupling measurements of transmembrane proteins using aligned low-q bicelles and high-resolution magic angle spinning NMR spectroscopy. *J. Am. Chem. Soc.* 130:13294–13300. <http://dx.doi.org/10.1021/ja802578z>
- Chaplan, S.R., F.W. Bach, J.W. Pogrel, J.M. Chung, and T.L. Yaksh. 1994. Quantitative assessment of tactile allodynia in the rat paw. *J. Neurosci. Methods.* 53:55–63. [http://dx.doi.org/10.1016/0165-0270\(94\)90144-9](http://dx.doi.org/10.1016/0165-0270(94)90144-9)
- Cheng, M.H., L.T. Liu, A.C. Saladino, Y. Xu, and P. Tang. 2007. Molecular dynamics simulations of ternary membrane mixture: phosphatidylcholine, phosphatidic acid, and cholesterol. *J. Phys. Chem. B.* 111:14186–14192. <http://dx.doi.org/10.1021/jp075467b>
- Costa, B. 2007. On the pharmacological properties of Delta9-tetrahydrocannabinol (THC). *Chem. Biodivers.* 4:1664–1677. <http://dx.doi.org/10.1002/cbdv.200790146>
- Costa, B., A.E. Trovato, F. Comelli, G. Giagnoni, and M. Colleoni. 2007. The non-psychoactive cannabis constituent cannabidiol is an orally effective therapeutic agent in rat chronic inflammatory and neuropathic pain. *Eur. J. Pharmacol.* 556:75–83. <http://dx.doi.org/10.1016/j.ejphar.2006.11.006>
- Delaglio, F., S. Grzesiek, G.W. Vuister, G. Zhu, J. Pfeifer, and A. Bax. 1995. NMRPipe: a multidimensional spectral processing system based on UNIX pipes. *J. Biomol. NMR.* 6:277–293. <http://dx.doi.org/10.1007/BF00197809>
- Demir, R., M. Leuwer, J. de la Roche, K. Krampfl, N. Foadi, M. Karst, R. Dengler, G. Haeseler, and J. Ahrens. 2009. Modulation of glycine receptor function by the synthetic cannabinoid HU210. *Pharmacology.* 83:270–274. <http://dx.doi.org/10.1159/000209291>
- Dixon, W.J. 1980. Efficient analysis of experimental observations. *Annu. Rev. Pharmacol. Toxicol.* 20:441–462. <http://dx.doi.org/10.1146/annurev.pa.20.040180.002301>
- Dobos, I., K. Toth, G. Kekesi, G. Joo, E. Csullog, W. Klimscha, G. Benedek, and G. Horvath. 2003. The significance of intrathecal catheter location in rats. *Anesth. Analg.* 96:487–492.
- Eswar, N., B. Webb, M.A. Marti-Renom, M.S. Madhusudhan, D. Eramian, M.Y. Shen, U. Pieper, and A. Sali. 2007. Comparative protein structure modeling using MODELLER. *Curr. Protoc. Protein Sci.* Chapter 2:Unit 2.9.
- Foadi, N., M. Leuwer, R. Demir, R. Dengler, V. Buchholz, J. de la Roche, M. Karst, G. Haeseler, and J. Ahrens. 2010. Lack of positive allosteric modulation of mutated alpha(1)S267I glycine receptors by cannabinoids. *Naunyn Schmiedebergs Arch. Pharmacol.* 381:477–482. <http://dx.doi.org/10.1007/s00210-010-0506-9>
- Grossman, M.L., A.I. Basbaum, and H.L. Fields. 1982. Afferent and efferent connections of the rat tail flick reflex (a model used to analyze pain control mechanisms). *J. Comp. Neurol.* 206:9–16. <http://dx.doi.org/10.1002/cne.902060103>
- Guan, Y., L.M. Johaneck, T.V. Hartke, B. Shim, Y.X. Tao, M. Ringkamp, R.A. Meyer, and S.N. Raja. 2008. Peripherally acting mu-opioid receptor agonist attenuates neuropathic pain in rats after L5 spinal nerve injury. *Pain.* 138:318–329. <http://dx.doi.org/10.1016/j.pain.2008.01.004>
- Hargreaves, K., R. Dubner, F. Brown, C. Flores, and J. Joris. 1988. A new and sensitive method for measuring thermal nociception in cutaneous hyperalgesia. *Pain.* 32:77–88. [http://dx.doi.org/10.1016/0304-3959\(88\)90026-7](http://dx.doi.org/10.1016/0304-3959(88)90026-7)
- Harrison, C. 2011. Analgesia: Inhibiting neuropathic pain. *Nat. Rev. Drug Discov.* 10:176. <http://dx.doi.org/10.1038/nrd3396>
- Harvey, R.J., U.B. Depner, H. Wässle, S. Ahmadi, C. Heindl, H. Reinold, T.G. Smart, K. Harvey, B. Schütz, O.M. Abo-Salem, et al. 2004. GlyR alpha3: an essential target for spinal PGE2-mediated inflammatory pain sensitization. *Science.* 304:884–887. <http://dx.doi.org/10.1126/science.1094925>
- Harvey, V.L., A. Caley, U.C. Müller, R.J. Harvey, and A.H. Dickenson. 2009. A selective role for alpha3 subunit glycine receptors in inflammatory pain. *Front. Mol. Neurosci.* 2:14. <http://dx.doi.org/10.3389/neuro.02.014.2009>
- Hejazi, N., C. Zhou, M. Oz, H. Sun, J.H. Ye, and L. Zhang. 2006. Delta9-tetrahydrocannabinol and endogenous cannabinoid anandamide directly potentiate the function of glycine receptors. *Mol. Pharmacol.* 69:991–997.
- Hösl, K., H. Reinold, R.J. Harvey, U. Müller, S. Narumiya, and H.U. Zeilhofer. 2006. Spinal prostaglandin E receptors of the EP2 subtype and the glycine receptor alpha3 subunit, which mediate central inflammatory hyperalgesia, do not contribute to pain after peripheral nerve injury or formalin injection. *Pain.* 126:46–53. <http://dx.doi.org/10.1016/j.pain.2006.06.011>
- Howlett, A.C., F. Barth, T.I. Bonner, G. Cabral, P. Casellas, W.A. Devane, C.C. Felder, M. Herkenham, K. Mackie, B.R. Martin, et al. 2002. International Union of Pharmacology. XXVII. Classification of cannabinoid receptors. *Pharmacol. Rev.* 54:161–202. <http://dx.doi.org/10.1124/pr.54.2.161>
- Huestis, M.A., and R.G. Pertwee. 2005. Pharmacokinetics and Metabolism of the Plant Cannabinoids, Δ9-Tetrahydrocannabinol, Cannabidiol and Cannabinol. Vol. 168. Springer Berlin, Heidelberg, Germany. 657 pp.
- Hyliden, J.L., and G.L. Wilcox. 1980. Intrathecal morphine in mice: a new technique. *Eur. J. Pharmacol.* 67:313–316. [http://dx.doi.org/10.1016/0014-2999\(80\)90515-4](http://dx.doi.org/10.1016/0014-2999(80)90515-4)
- Izzo, A.A., F. Borrelli, R. Capasso, V. Di Marzo, and R. Mechoulam. 2009. Non-psychoactive plant cannabinoids: new therapeutic opportunities from an ancient herb. *Trends Pharmacol. Sci.* 30:515–527. <http://dx.doi.org/10.1016/j.tips.2009.07.006>
- Liu, Z.W., Y. Xu, A.C. Saladino, T. Wymore, and P. Tang. 2004. Parametrization of 2-bromo-2-chloro-1,1,1-trifluoroethane (halothane) and hexafluoroethane for nonbonded interactions. *J. Phys. Chem. A.* 108:781–786. <http://dx.doi.org/10.1021/jp0368482>
- Lynch, J.W. 2004. Molecular structure and function of the glycine receptor chloride channel. *Physiol. Rev.* 84:1051–1095. <http://dx.doi.org/10.1152/physrev.00042.2003>
- Lynch, J.W., and R.J. Callister. 2006. Glycine receptors: a new therapeutic target in pain pathways. *Curr. Opin. Investig. Drugs.* 7:48–53.

- Lynch, M.E., and F.Campbell. 2011. Cannabinoids for treatment of chronic non-cancer pain; a systematic review of randomized trials. *Br. J. Clin. Pharmacol.* 72:735–744. <http://dx.doi.org/10.1111/j.1365-2125.2011.03970.x>
- Ma, D., Z. Liu, L. Li, P. Tang, and Y. Xu. 2005. Structure and dynamics of the second and third transmembrane domains of human glycine receptor. *Biochemistry.* 44:8790–8800. <http://dx.doi.org/10.1021/bi050256n>
- Manzke, T., M. Niebert, U.R. Koch, A. Caley, S. Vogelgesang, S. Hülsmann, E. Ponimaskin, U. Müller, T.G. Smart, R.J. Harvey, and D.W. Richter. 2010. Serotonin receptor 1A-modulated phosphorylation of glycine receptor $\alpha 3$ controls breathing in mice. *J. Clin. Invest.* 120:4118–4128. <http://dx.doi.org/10.1172/JCI43029>
- Marchand, F., M. Perretti, and S.B. McMahon. 2005. Role of the immune system in chronic pain. *Nat. Rev. Neurosci.* 6:521–532. <http://dx.doi.org/10.1038/nrn1700>
- Mogil, J.S. 2009. Animal models of pain: progress and challenges. *Nat. Rev. Neurosci.* 10:283–294. <http://dx.doi.org/10.1038/nrn2606>
- Möller, C., and M.S. Plesset. 1934. Note on an approximation treatment for many-electron systems. *Physical Review.* 46:618–622. <http://dx.doi.org/10.1103/PhysRev.46.618>
- Morris, G.M., D.S. Goodsell, R.S. Halliday, R. Huey, W.E. Hart, R.K. Belew, and A.J. Olson. 1998. Automated docking using a Lamarckian genetic algorithm and an empirical binding free energy function. *J. Comput. Chem.* 19:1639–1662. [http://dx.doi.org/10.1002/\(SICI\)1096-987X\(19981115\)19:14<1639::AID-JCC10>3.0.CO;2-B](http://dx.doi.org/10.1002/(SICI)1096-987X(19981115)19:14<1639::AID-JCC10>3.0.CO;2-B)
- Murray, R.M., P.D. Morrison, C. Henquet, and M. Di Forti. 2007. Cannabis, the mind and society: the hash realities. *Nat. Rev. Neurosci.* 8:885–895. <http://dx.doi.org/10.1038/nrn2253>
- Nurmikko, T.J., M.G. Serpell, B. Hoggart, P.J. Toomey, B.J. Morlion, and D. Haines. 2007. Sativex successfully treats neuropathic pain characterised by allodynia: a randomised, double-blind, placebo-controlled clinical trial. *Pain.* 133:210–220. <http://dx.doi.org/10.1016/j.pain.2007.08.028>
- Pan, Y.Z., and H.L. Pan. 2004. Primary afferent stimulation differentially potentiates excitatory and inhibitory inputs to spinal lamina II outer and inner neurons. *J. Neurophysiol.* 91:2413–2421. <http://dx.doi.org/10.1152/jn.01242.2003>
- Patapoutian, A., S. Tate, and C.J. Woolf. 2009. Transient receptor potential channels: targeting pain at the source. *Nat. Rev. Drug Discov.* 8:55–68. <http://dx.doi.org/10.1038/nrd2757>
- Pernía-Andrade, A.J., A. Kato, R. Witschi, R. Nyilas, I. Katona, T.F. Freund, M. Watanabe, J. Filitz, W. Koppert, J. Schüttler, et al. 2009. Spinal endocannabinoids and CB1 receptors mediate C-fiber-induced heterosynaptic pain sensitization. *Science.* 325:760–764. <http://dx.doi.org/10.1126/science.1171870>
- Phillips, J.C., R. Braun, W. Wang, J. Gumbart, E. Tajkhorshid, E. Villa, C. Chipot, R.D. Skeel, L. Kalé, and K. Schulten. 2005. Scalable molecular dynamics with NAMD. *J. Comput. Chem.* 26:1781–1802. <http://dx.doi.org/10.1002/jcc.20289>
- Saladino, A.C., and P. Tang. 2004. Optimization of structures and LJ parameters of 1-chloro-1,2,2-trifluorocyclobutane and 1,2-dichlorohexafluorocyclobutane. *J. Phys. Chem. A.* 108:10560–10564. <http://dx.doi.org/10.1021/jp046662i>
- Turcotte, D., J.A. Le Dorze, F. Esfahani, E. Frost, A. Gomori, and M. Namaka. 2010. Examining the roles of cannabinoids in pain and other therapeutic indications: a review. *Expert Opin. Pharmacother.* 11:17–31. <http://dx.doi.org/10.1517/14656560903413534>
- Vanegas, H., and H.G. Schaible. 2001. Prostaglandins and cyclooxygenases [correction of cyclooxygenases] in the spinal cord. *Prog. Neurobiol.* 64:327–363. [http://dx.doi.org/10.1016/S0301-0082\(00\)00063-0](http://dx.doi.org/10.1016/S0301-0082(00)00063-0)
- Vanommeslaeghe, K., E. Hatcher, C. Acharya, S. Kundu, S. Zhong, J. Shim, E. Darian, O. Guvench, P. Lopes, I. Vorobyov, and A.D. Mackerell Jr. 2010. CHARMM general force field: A force field for drug-like molecules compatible with the CHARMM all-atom additive biological force fields. *J. Comput. Chem.* 31:671–690.
- Xiong, W., M. Hosoi, B.N. Koo, and L. Zhang. 2008. Anandamide inhibition of 5-HT_{3A} receptors varies with receptor density and desensitization. *Mol. Pharmacol.* 73:314–322. <http://dx.doi.org/10.1124/mol.107.039149>
- Xiong, W., K. Cheng, T. Cui, G. Godlewski, K.C. Rice, Y. Xu, and L. Zhang. 2011. Cannabinoid potentiation of glycine receptors contributes to cannabis-induced analgesia. *Nat. Chem. Biol.* 7:296–303. <http://dx.doi.org/10.1038/nchembio.552>
- Xiong, W., X. Wu, D.M. Lovinger, and L. Zhang. 2012. A common molecular basis for exogenous and endogenous cannabinoid potentiation of glycine receptors. *J. Neurosci.* 32:5200–5208. <http://dx.doi.org/10.1523/JNEUROSCI.6347-11.2012>
- Yang, Z., K.R. Aubrey, I. Alroy, R.J. Harvey, R.J. Vandenberg, and J.W. Lynch. 2008. Subunit-specific modulation of glycine receptors by cannabinoids and N-arachidonyl-glycine. *Biochem. Pharmacol.* 76:1014–1023. <http://dx.doi.org/10.1016/j.bcp.2008.07.037>
- Yevenes, G.E., and H.U. Zeilhofer. 2011a. Allosteric modulation of glycine receptors. *Br. J. Pharmacol.* 164:224–236. <http://dx.doi.org/10.1111/j.1476-5381.2011.01471.x>
- Yevenes, G.E., and H.U. Zeilhofer. 2011b. Molecular sites for the positive allosteric modulation of glycine receptors by endocannabinoids. *PLoS ONE.* 6:e23886. <http://dx.doi.org/10.1371/journal.pone.0023886>
- Zeilhofer, H.U. 2005. The glycinergic control of spinal pain processing. *Cell. Mol. Life Sci.* 62:2027–2035. <http://dx.doi.org/10.1007/s00018-005-5107-2>
- Zeilhofer, H.U., D. Benke, and G.E. Yevenes. 2012. Chronic pain States: pharmacological strategies to restore diminished inhibitory spinal pain control. *Annu. Rev. Pharmacol. Toxicol.* 52:111–133. <http://dx.doi.org/10.1146/annurev-pharmtox-010611-134636>
- Zhang, G., W. Chen, L. Lao, and J.C. Marvizón. 2010. Cannabinoid CB1 receptor facilitation of substance P release in the rat spinal cord, measured as neurokinin 1 receptor internalization. *Eur. J. Neurosci.* 31:225–237. <http://dx.doi.org/10.1111/j.1460-9568.2009.07075.x>
- Zhou, H.Y., H.M. Zhang, S.R. Chen, and H.L. Pan. 2008. Increased C-fiber nociceptive input potentiates inhibitory glycinergic transmission in the spinal dorsal horn. *J. Pharmacol. Exp. Ther.* 324:1000–1010. <http://dx.doi.org/10.1124/jpet.107.133470>
- Zhuo, M. 2007. Neuronal mechanism for neuropathic pain. *Mol. Pain.* 3:14. <http://dx.doi.org/10.1186/1744-8069-3-14>
- Zimmer, A., A.M. Zimmer, A.G. Hohmann, M. Herkenham, and T.I. Bonner. 1999. Increased mortality, hypoactivity, and hypoalgesia in cannabinoid CB1 receptor knockout mice. *Proc. Natl. Acad. Sci. USA.* 96:5780–5785. <http://dx.doi.org/10.1073/pnas.96.10.5780>